# Compact deep-space optical communications transceiver

W. Thomas Roberts and Jeffrey R. Charles
Jet Propulsion Laboratory, California Institute of Technology, 4800 Oak Grove Dr., Pasadena, CA USA 91109

## ABSTRACT

Deep space optical communication transceivers must be very efficient receivers and transmitters of optical communication signals. For deep space missions, communication systems require high performance well beyond the scope of mere power efficiency, demanding maximum performance in relation to the precious and limited mass, volume, and power allocated. This paper describes the opto-mechanical design of a compact, efficient, functional brassboard deep space transceiver that is capable of achieving Mb/s rates at Mars ranges. The special features embodied to enhance the system operability and functionality, and to reduce the mass and volume of the system are detailed. System tests and performance characteristics are described in detail. Finally, lessons learned in the implementation of the brassboard design and suggestions for improvements appropriate for a flight prototype are covered.

**Keywords**: Optical Communications, Optical Transceiver, DSOCT, Deep-Space Transceiver

## 1. INTRODUCTION

Deep-space optical communications transceivers capable of efficiently transmitting data rates of several Mb/s from interplanetary ranges have been considered for over 2 decades [1]. A 28 cm flight transceiver called the Optical Transceiver Package was designed in the early 1980's to transmit 100 kbps from Saturn, though it was never built [2]. The 10 cm Optical Communications Demonstrator (OCD) was designed, built and operationally demonstrated a decade later, based on a simplified design concept [3-5]. Earlier this decade, the Mars Laser Communication Demonstration (MLCD) project designed a 30 cm flight transceiver capable of 10's of Mb/s communication rates from Mars [6]. Budgetary constraints forced cancellation of the spacecraft and the demonstration before the transceiver could be prototyped and tested.

In an effort to keep up with the development of new technology bringing the potential of interplanetary optical communications closer to reality, we have undertaken the task of developing a flight-like transceiver employing these technical advances, thus reducing the risk of employing an optical communications transceiver on a near-term Mars spacecraft.

The new technology around which this system is designed consists of (1) medium-format photon-counting detector arrays capable of signal recovery from a modulated beacon, (2) flight qualified piezo-actuated steering mirrors, (3) two-photon absorption in silicon for observing the angle of a downlink 1550 nm signal relative to the beacon, and (4) a sub-Hertz stabilization platform eliminating the need for a fast-steering mirror. The details of the system and more are covered in [7] in this volume.

## 2. SYSTEM DESIGN REQUIREMENTS

There are many similarities between the design of deep-space optical communications transceivers and space-based imaging telescopes; both generally use diffraction-limited optics; both require the use of flight-qualifiable materials; both must mechanically survive the venting, vibration and acceleration of launch, and either maintain alignment through this environment and in the micro-gravity environment of space, or have systems and controls to allow the recovery of alignment once the system is on station.

Free-Space Laser Communication Technologies XXI, edited by Hamid Hemmati,
Proc. of SPIE Vol. 7199, 71990L · © 2009 SPIE · CCC code: 0277-786X/09/$18 · doi: 10.1117/12.806290

Optical communications transceivers have certain requirements that are more readily achieved than their corresponding requirements on space-based astronomical telescopes. One example is that the field of view of a deep-space optical transceiver is frequently smaller than that of an imaging telescope; it generally only needs to be about twice the maximum point-ahead angle. This angle is 2 $v_p/c$, where $v_p$ is the planet's linear velocity perpendicular to the communication line-of-sight, and c is the speed of light. For interplanetary communications, Mars presents the most stressing field requirements, requiring a field of about 400 μrad. Even then the system does not necessarily need to be diffraction-limited across the field, as long as the beacon source can be detected and its position adequately derived (by centroiding or calibration) at angles up to the maximum point-ahead angle.

To maximize the efficiency of mass and volume for the system, and to minimize any transmit/receive alignment concerns, a deep-space optical communications terminal employs the same telescope for both reception of the uplink beacon, and transmission of the downlink signal. This imposes a requirement on transmit/receive isolation which must be achieved through some combination of polarization separation, spectral separation (e.g. dichroic beamsplitters or diffraction gratings) and angular separation (e.g. field stops) to generate isolations of greater than 100 dB.

An important difference between the design of an optical communications terminal and a space-based imaging telescope is that, while the telescope can be designed for a restricted thermal environment (such as always sun-pointing for a solar telescope, or never sun-pointing for a low background observatory), an optical communications transceiver must cover an extended range, since it must periodically point throughout the ecliptic plane. Maintaining communications near solar conjunction is very difficult; not only is the range near its maximum under these conditions requiring the maximum system sensitivity, but scattered solar background light and thermal effects leading to telescope misalignment are at their worst.

Finally, this is an attempt to build a 'flight-like' transceiver to demonstrate system functionality and experiment with the transceiver's performance under widely varying conditions. However, it is still subject to budget and schedule constraints more akin to research projects than to building a true flight transceiver. As a result, the design must incorporate the use of off-the-shelf parts as much as possible, while still selecting flight qualifiable (though not flight qualified) components to assure proper functionality and similar performance. This constraint primarily comes into play in the selection of lenses and beamsplitters, for which off-the-shelf multi-element lenses might be used. In a true flight instrument, these would be replaced by custom manufactured and tested lenses.

Table 1 Top-level design requirements for Deep-Space Optical Communications Transceiver

| **Parameter** | **Requirement** | **Rationale** |
|---|---|---|
| Aperture | 15 cm | Achieve link goals (multiple Mb/s from Mars) in small package |
| Focal Length | 2500 mm | Provides a 400 μrad FOV using a 2 mm focal plane array |
| Telescope Magnification | ~10:1 | Allows limited throw of the Point Ahead Mirror to address full FOV |
| Linear Obscuration | ~35% | Maintain a far-field obscuration loss of less than 2 dB [8] while controlling coma |
| Transmit Wavelength | 1550 nm | Leverage off of efficient telecom laser development |
| Receive Wavelength | 1060 nm | Allows the use of high-power ground based beacon lasers and provides for good transmit/receive isolation |
| Strehl Ratio | >0.2 | Allows detection of the beacon across the full FOV |
| Solar Environment | Full Range | Must be able to survive direct Sun pointing, operate at peak performance within 3 degrees of Sun, and operate while pointing at opposition |

# 3. OPTICAL DESIGN OF THE DEEP-SPACE OPTICAL COMMUNICATIONS TRANSCEIVER

The Deep-Space Optical Communications Transceiver is conveniently divided into two separate parts: a front telescope optical system followed by an aft-optics beam management system (Figure 1). The design began independently, *i.e.* by generating a good diffraction-limited telescope independently of a good first-order aft-optics module. The latter's use of off-the-shelf optical components primarily designed for the visible spectrum led to significant aberration when employed at the 1060 nm and 1550 nm wavelengths and in the desired imaging configuration. The final step in the design was to adjust the specifics of the telescope (notably the conic constant and radius of curvature of the secondary mirror) to compensate for the residual aberrations of the aft optics.

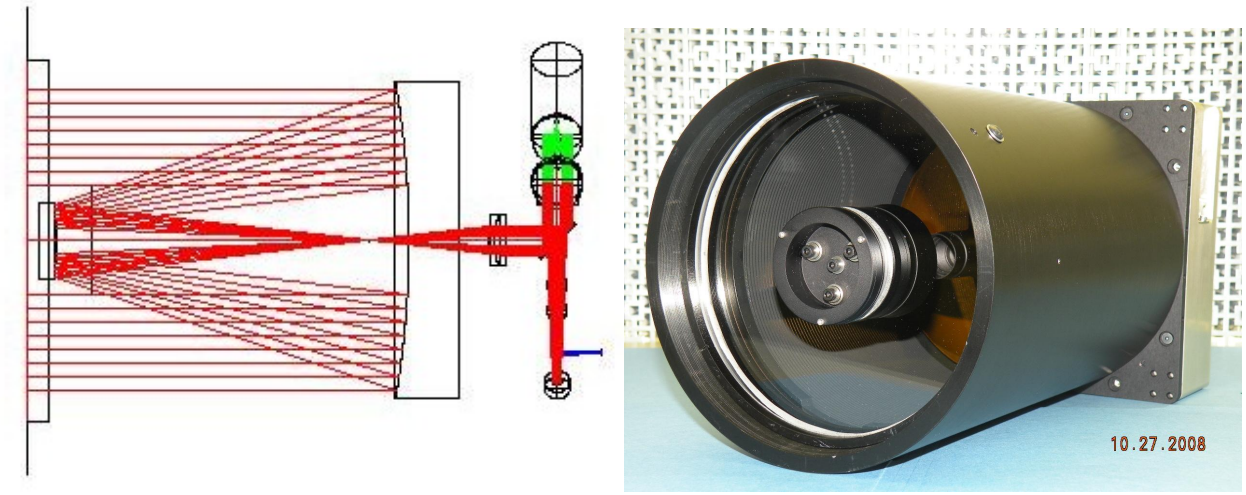


Fig. 1 Side view of the DSOCT. Optical drawing (left): Collimated light from the far field enters at left, passes through the solar window, and reflects from the primary and secondary mirrors. After coming to focus at the field stop, the light is then collimated by a doublet lens, and is then reflected into the aft-optics plane, mounted transverse to the telescope axis. Assembled instrument (right).

### 3.1 Telescope Assembly

The goal of the front optics system is to provide an optical telescope with a relatively long focal length (~2.5 m), but a short physical length to keep the system's volume and mass low. A Cassegrain-type optical telescope was designed to place the focus in front of the primary mirror vertex to allow the beam to expand to a collimating doublet placed just beyond the back of the primary mirror. The telescope design results in a system with focal ratio of F/4.2 and an effective focal length of 626 mm.

To maintain a more stable thermal environment and provide for a spiderless mounting surface for the secondary mirror assembly, a flat glass filter is placed just outside the secondary mirror assembly. The filter is tilted slightly to prevent back-reflection of the transmitted laser into the optical system. The filter's front surface is coated with a multilayer dielectric coating designed to reflect most of the visible radiation from the Sun, while efficiently transmitting 94% of the uplink beam at 1060 nm and >96% of the downlink beam at 1550 nm. The filter was intentionally designed to transmit a slight amount of visible light to aid in telescope assembly and alignment. Overall, the filter is measured to reject about 80% of the exoatmospheric solar spectrum, providing substantial thermal protection for the telescope assembly.

In addition to controlling the telescope's thermal environment under solar loading, the filter is expected to aid in suppressing some of the solar-generated background light from sunlight coming in from larger off-axis angles (> 20° off axis). This occurs because the angle-tuning of thin-film layers shifts the transmission bands to shorter wavelengths which are highly attenuated by filters in the aft-optics assembly. Finally, the optical filter protects the remainder of the optical elements from contamination, providing a flat, unpowered surface, which can be cleaned prior to flight, and reducing the total amount of exposed surface to collect contamination while on station.

### 3.2 Aft-optics assembly

The portion of the optical design behind the collimating lens of the Cassegrain telescope, the 'aft optics', is designed to integrate three separate optical channels: a transmit channel to transmit a diffraction-limited 1550 nm beam, a tracking channel, to precisely determine the angular location of the uplink beacon and the relative pointing of the downlink signal, and an auxiliary receive channel for testing the system with externally-mounted camera systems. These three channels are all designed to use the full aperture of the main telescope, and all fit within a box that inscribes the telescope body.

The aft-optics assembly is canted from the vertical line to fit the relatively large point-ahead mirror actuator, shown in the upper right of the figure. The receive beam is brought back into alignment with the sides of the aft-optics box to allow for wander-free focusing of an auxiliary camera system which would usually be mounted normal to the box surface.

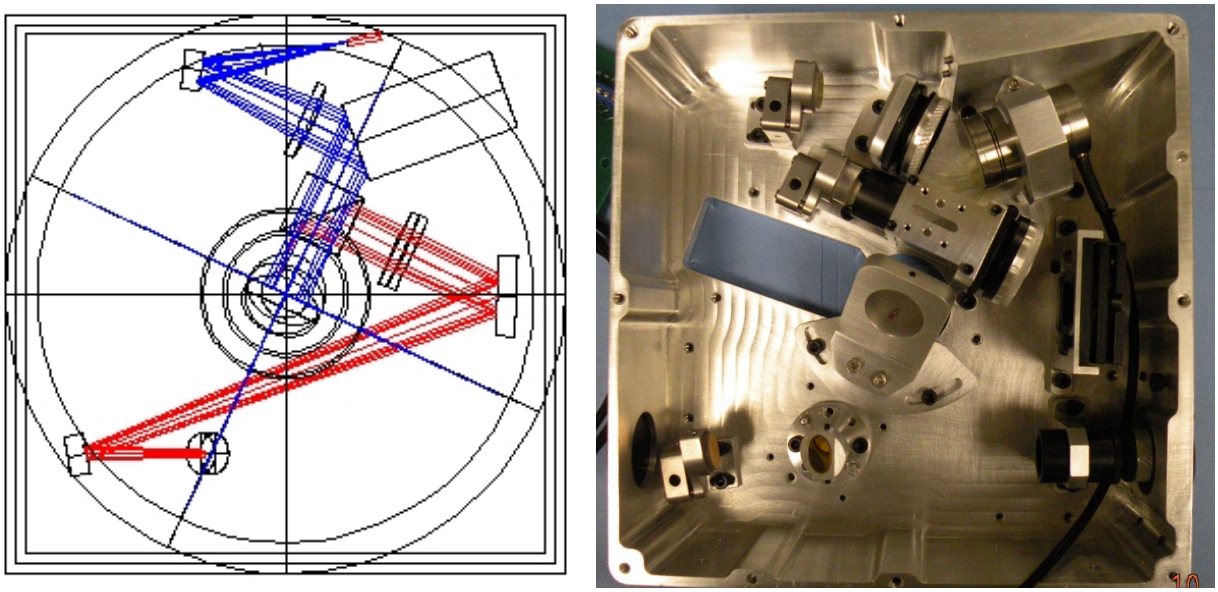

Fig. 2 Aft-optics assembly optical drawing (left) and photo (right), showing the laser path (top) and the receive path (bottom). The retro-assembly directing a small fraction of the emitted laser light toward the receive channel is not shown. The final leg of the receive channel is directed up, out of the plane of the page, into the focal plane array which is connected to the aft electronics assembly.

#### 3.2.1 Transmit Channel

The laser channel is designed for use with a multi-Watt pulse position modulated fiber laser. The laser driver and downlink encoder is housed separate from the telescope assembly to minimize power dissipation in the telescope assembly. The fiber input is an angled receptacle recessed into the otherwise square body of the transceiver to minimize strain on the fiber and reduce the overall footprint of the transceiver. Light diverges from the single-mode fiber, and reflects from a high-efficiency protected gold mirror into a collimating Gradium (gradient index) lens. From there, the collimated beam reflects from a piezo-actuated Point Ahead Mirror (PAM), which generates the point-ahead angle between the observed beacon and the downlink beam.

After reflecting from the PAM, the collimated beam transmits, largely undisturbed and unattenuated, through a dichroic beamsplitter cube, which performs the bulk of the transmit/receive channel separation. The transmitted beam is then reflected from a fold mirror at the center of the aft-optics module, into the back of the telescope.

A small fraction (<0.5%) of the transmitted beam is reflected from the angled fold surface in the dichroic beamsplitter cube. Because the propagation direction of the beam is opposite that of the incoming beam, it is reflected away from the receive channel. However, this light is considered useful as a means of monitoring and correcting the transmission direction, so it is reflected back into the receive channel where the collimated beam is focused onto the tracking array. Even though the tracking array is fabricated from silicon, which cannot directly detect 1550 nm photons, the spot can be observed through non-linear two-photon absorption. This process is sufficiently efficient to require attenuation filters to

reduce the intensity of the monitored 1550 nm spot on the tracking array. Though the receive channel was optimized for diffraction-limited performance at 1060 nm, the 1550 nm spot is likewise corrected to diffraction-limited performance by introducing a slight curvature to the return mirror.

### 3.2.2 Tracking Channel

The operational concept calls for the system to observe and lock-in on a beacon from Earth to serve as a reference for pointing the narrow transmit beam. Uplink information can be encoded on this beacon, and must be detected and decoded by the DSOCT. These functions are performed in the tracking channel, which must observe the point-ahead field and identify the location of the reference signal. This is done by focusing the collimated 1060 nm reference signal onto an 80x80 array of 24 μm silicon pixels. An off-the-shelf achromatic doublet was used to generate the focus providing a 378 x 378 μrad field of view. The long focus of this channel is accommodated by using three fold mirrors to reflect the beam around the cavity and up into the focal plane array which is physically attached to the aft electronics box. A telephoto system was considered for reducing the physical length of this channel, but added cost and complexity, and did not match the optical performance of the folded system.

### 3.2.3 Auxiliary Tracking Channel

An auxiliary tracking channel was designed into the system to aid in using the transceiver as a testbed for other tracking sensors. This channel requires removal of the final fold mirror, allowing the beam to come to a focus past the nominal location of this mirror. A pair of identical achromatic doublets then collimates and reimages the far field onto a plane beyond the outer housing surface to allow for the attachment of a standard C-mount camera.

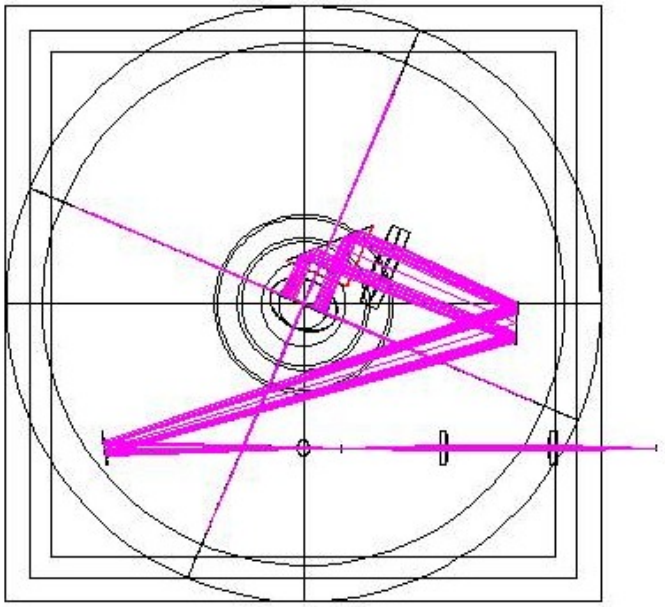

Fig. 3 Auxiliary channel allowing connection of an external camera to the side of the instrument. Operation in this channel requires removal of the fourth fold mirror to allow the beam access to the collimating and focusing lenses shown.

## 4. OPTICAL SYSTEM MANUFACTURING

The manufacturer's approach began with fabrication of a paraboloidal primary mirror with a base curvature within a few mm of the specified radius. Next a spherical secondary mirror (without the conic figured into it) was placed at the appropriate distance from the primary mirror vertex, and was iteratively polished until it produced a good on-axis spot at the telescope focus. Final figuring of the secondary mirror was completed with the aid of the collimating and focusing doublet lenses used in the transceiver. By placing these lenses at the appropriate locations (Figure 4), the secondary mirror was polished until the spot generated by the combined telescope and aft-optics lenses was sufficiently small to be diffraction limited at 1060 nm.

While the system was intended for use in the near IR, all manufacturing was done using a 532 nm collimated laser input. Dispersion in the lenses would therefore result in significant focal shifts and consequent aberration effects at the focal plane. This was considered, and modeled using ZEMAX to assure that the telescope produced by this method would still meet the requirements at the correct wavelengths. In this analysis, the figures of all of the elements were held constant: only spacings between separate elements were allowed to vary. The input wavelength was set to 532 nm, and the spacings among the transmitting elements, focal plane and field stop were optimized for the new wavelength. These spacings were then fixed, and the radius of curvature and conic constant of the secondary mirror were set as variables, which were then optimized against an RMS spot size merit function. The resulting secondary mirror was assumed to have the figure that the vendor would generate through his stated test method. As expected, the resulting secondary mirror figure varied from the design slightly in both base radius and conic constant. To determine that the primary and secondary mirrors 'as produced' would be able to meet the optical requirements, the wavelength was set back to 1060 nm, and the spacings of the elements were once again optimized against the RMS spot size merit function. The resultant system was slightly different from the originally specified system, but virtually identical in performance at the 1060 nm wavelength of intended use.

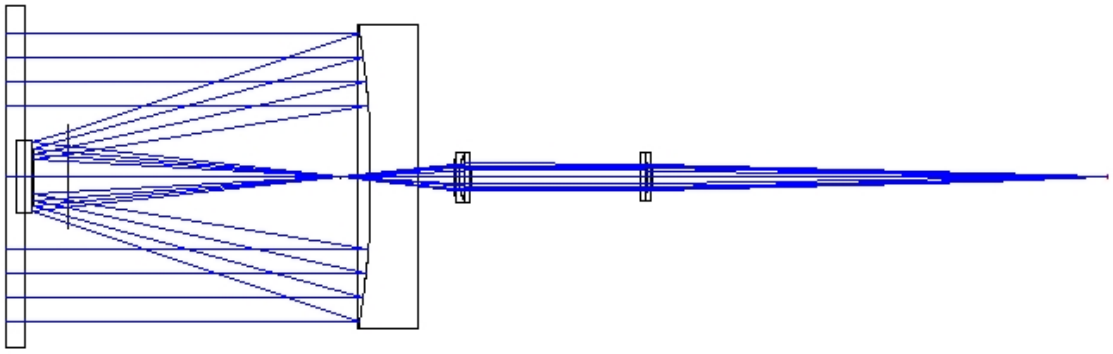

Fig. 4 Manufacturing and testing setup, showing primary and secondary mirrors, beam collimating lens, and final focusing lens.

## 5. TEST RESULTS

The telescope assembly, comprised of the solar window, the primary and secondary mirrors, and the collimating doublet, were assembled and tested using a collimated 633 nm laser source. The collimated output of the telescope assembly was focused to a spot using an independent Maksutov telescope, focused and characterized using the same collimated source. The disappointing resultant spot image is shown in Figure 5 below.

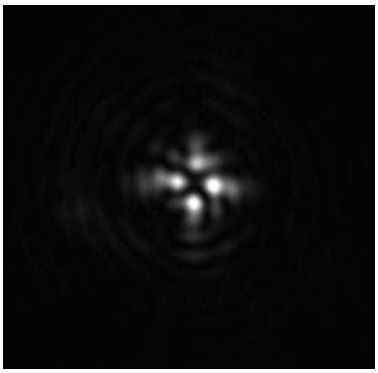

Figure 5 Best spot obtained with the telescope as produced. The telescope observed here was comprised of the solar filter, the primary and secondary mirrors, and the collimating doublet described in the text. The size of each lobe observed in the image is roughly the size of the expected Airy disk.

Significant effort was expended to try to improve the spot image: translation and tilting of the secondary mirror with respect to the primary mirror, along with off-axis use of the entire telescope with respect to the incoming collimated beam were explored. None of these efforts, applied individually or in combination improved the image beyond that shown above.

The simplest explanation of this pattern is obtained by assuming a slight degree of spherical aberration (expected because we were testing at 633 nm using doublets in a system designed for use at 1060 nm) combined with an azimuthal asymmetry of the primary mirror (an effect in which the x and y axes exhibit different curvatures and conic constants, sometimes referred to as 'astigmatism'). Along one axis, the primary curvature under-corrects the spherical aberration, while along the orthogonal axis it over-corrects. Some evidence of the azimuthal asymmetry in the primary mirror is observed in the Foucault test image shown in Figure 6 below.

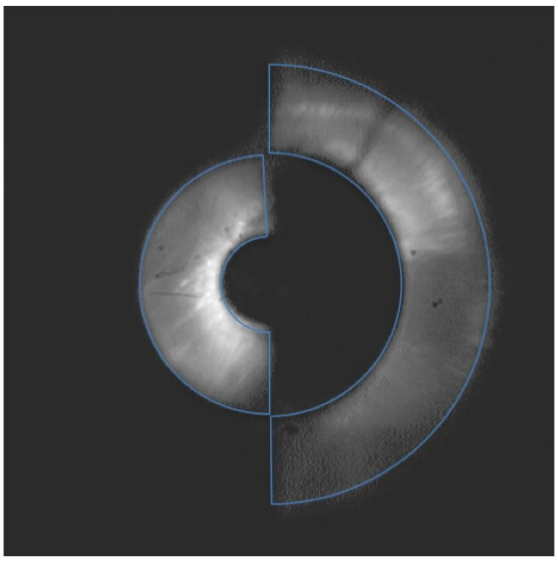

Fig. 6 Foucault (knife-edge) test of primary mirror. Note the slight departure of the image from the reference lines near the 1-o'clock and 6-o'clock positions.

This situation was modeled in ZEMAX using all elements at their nominal positions and in their 'perfect' configurations except for the primary mirror. The primary mirror was modeled as a biconic surface, changing the radius of curvature from 457.00 mm in both dimensions to 457.04 mm in x and 456.96 mm in the y dimension. The conic constant was changed from -1.00 in both dimensions to -1.02 in x and -0.98 in y. The resultant spot diagram (shown in Figure 7 below) was diamond-shaped and very similar to the observed spot, but the true similarity was not apparent until the Physical Optics Propagator in ZEMAX was used, which accounts for diffraction around apertures and interference of waves. Comparison of the physical optics model with the observed spot show remarkably good correspondence.

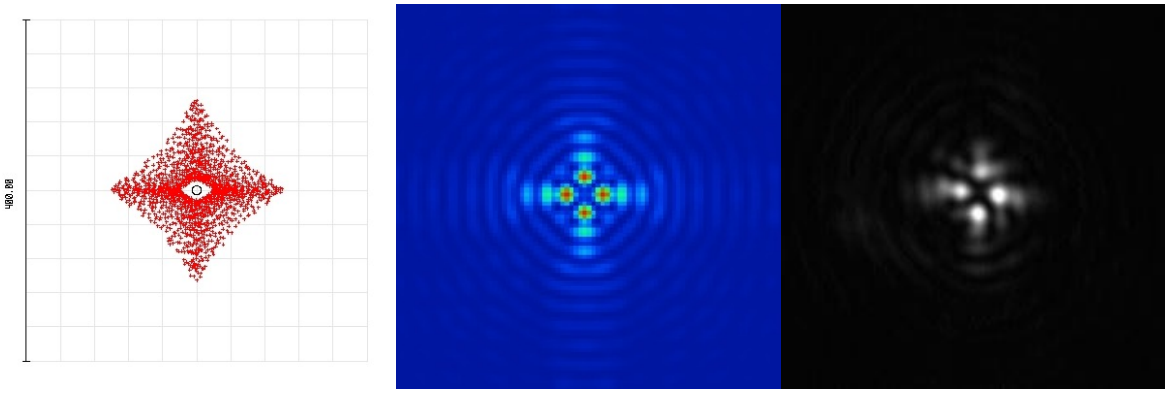

Fig. 7 Modeling of observed PSF. Left: Geometric ray trace spot resulting from slight changes to primary mirror ROC and conic constant. Center: Corresponding physical optics model. Right: Observed spot.

With some confidence that we understood the problems of the optical system as fabricated, we undertook to attempt to 'warp' the primary mirror. The primary is a thick piece of Pyrex glass, so it should not warp very easily; however, our modeling indicated that not much change to the surface was required to achieve a better result, so we applied pressure at the top and bottom of the y-axis using rounded-end screws threaded through the telescope assembly base plate. With only a slight amount of pressure applied (*i.e.* the mirror-warping screws were only tightened to 'finger-tight') the telescope point spread function changed to that shown in Figure 8 below. Obviously, this solution would not be acceptable for a flight instrument.

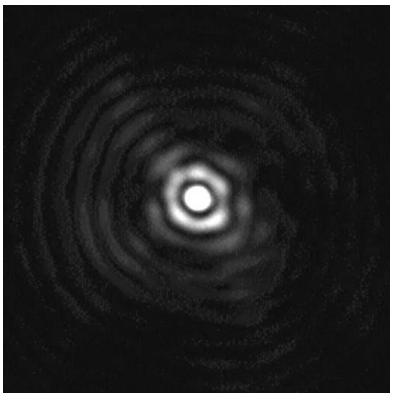

Fig. 8 Telescope point spread function after physically warping the primary mirror.

## 6. OPTO-MECHANICAL FEATURES

### 6.1. Baffle Design

Keeping background light at a minimum is a primary consideration in the design of deep-space transceivers; they frequently must operate in conditions in which the telescope is pointing to within a few degrees of the Sun. To accomplish this, the optical design performs a high degree of separation between the exposed telescope portion of the system and the light-tight aft-optics module. The only path through which scattered light in the solar-illuminated telescope portion of the system can enter the aft-optics module is through the 1.0 mm pinhole field stop placed between the primary and secondary mirror.

First order (single scatter) off-axis light transiting the field stop must come from either (1) light scattered into the telescope's FOV from a directly-illuminated optical surface, or (2) light scattered or diffracted from a surface within the direct FOV of the field stop. Reducing stray light from optical surfaces is achieved by (1) using fewer surfaces, (2) establishing and manufacturing to low roughness specifications, and (3) maintaining strict cleanliness standards. There is some debate over whether the inclusion of the solar rejection filter will increase or reduce the amount of in-band scattered radiance. The filter provides two additional surfaces to collect contaminants and to scatter through intrinsic surface roughness. These surfaces reside at the front of the telescope, and will be directly illuminated for Sun positions anywhere within the 180° angle in front of the telescope. Unless high-quality glass is used, the potential also exists for bulk scatter from impurities in the glass and glass striae. On the other hand, the filter effectively limits the exposure of its inner surface and the primary and secondary mirrors to particulate and aerosol contamination, and presents an easily-accessible flat surface which can be cleaned right up to launch. It has also been argued that scatter from particulate contamination on a transmission surface is limited to only forward scattering, whereas scatter from particulates on a reflective surface will have contributions from both forward and backward scattering. We hope that experimentation with this prototype will help to resolve some of these questions in the near future.

The objective of baffle design is to eliminate the second source of scatter outlined above: scatter or diffraction from a surface outside the nominal pupil of the telescope, but with a direct view of the field stop. Grazing-incidence reflections are known to be one of the most concerning types of scatter, primarily because of their potentially high magnitude. To reduce this, the inner surface of the primary baffle tube was machined with a reverse saw-tooth, presenting surfaces normal to the optical axis when viewed from inside, but sloped with respect to the axis when viewed from outside. This

sloping is intended to limit back-reflections onto the field of view from reflected solar irradiation and reflections from the transmitted laser.

A conical baffle surrounds the secondary mirror, partially protecting the secondary from off-axis scatter from inside the tube, but also protecting the primary baffle-tube extension from direct solar illumination. It is this baffle tube extension that we expect to provide the highest degree of stray light reduction. The extension effectively limits all single-scatter paths to the field stop, and eliminates most secondary-scatter paths as well through a series of sequentially narrower baffle rings.

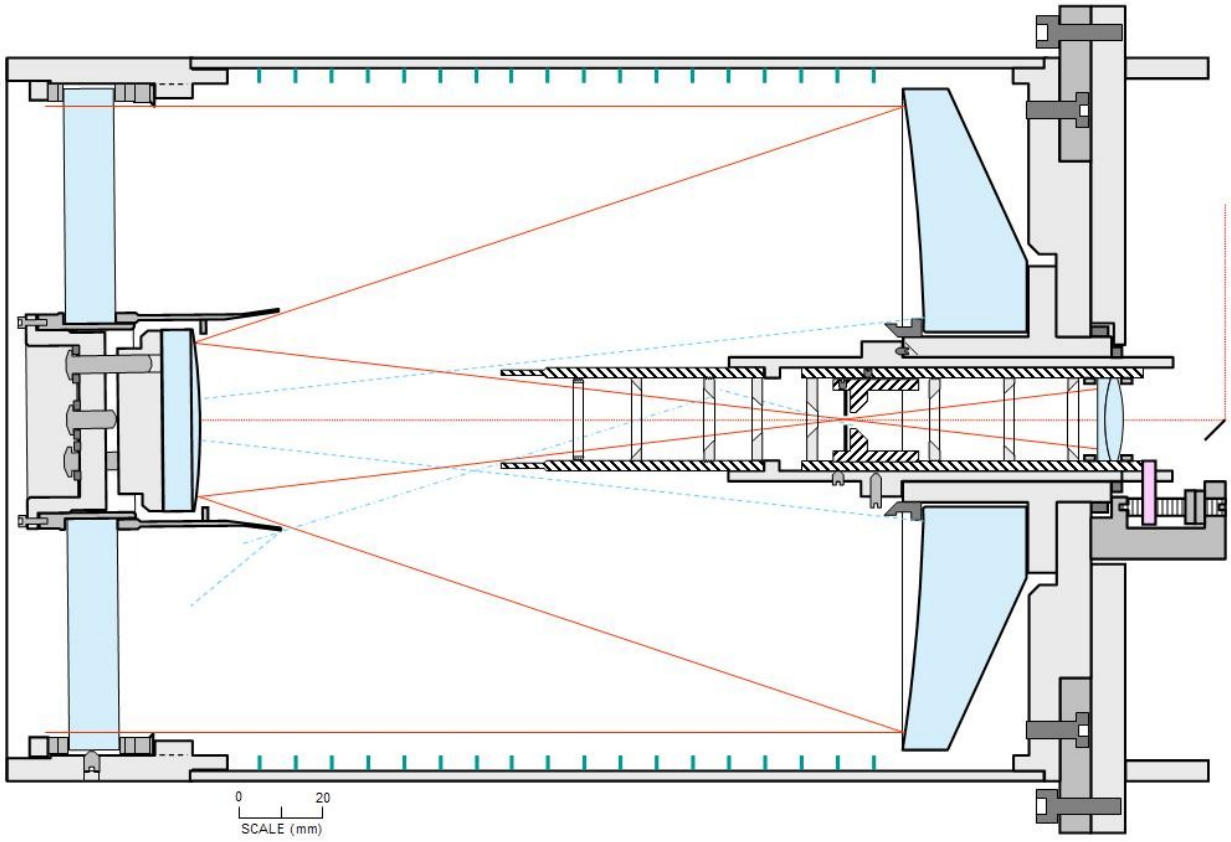


Fig. 9 Effective light baffling is accomplished via a baffled main tube, a primary baffle tube (projecting from the center of the primary mirror on the right), a secondary baffle tube (surrounding the secondary mirror at left), a series of baffle stops within each baffle tube, and a 1-mm field stop.

The light baffles are also designed to minimize retro-reflection of the transmit laser back into the system. Features facilitating this include a baffle stop around the inner (unused) zones of the primary mirror and chamfered baffle stops within the primary baffle tube. Combined with a 15 mm aperture stop for the transmit laser in the aft optics, these features substantially reduce unwanted retro-reflection of the transmit laser.

In addition to the baffles, the solar filter is tilted to prevent retro-reflection of the transmit laser back through the field stop. We have considered adding a dark spot or angled reflector to the center of the secondary mirror to further reduce retro-reflection, but will perform tests without this feature before deciding whether or not to implement it.

### 6.2. Focus mechanism

Even though a focus mechanism having significant travel is not a feature found on a typical space transceiver, a number of concerns dictated that focus capability would be appropriate for the brassboard telescope. These concerns included:

* Accommodating tests at different wavelengths, specifically at visible wavelengths, which are shorter than the transmit and receive wavelengths.

* Providing a means to fine-tune the spot size by accommodating the different Cassegrain focus locations obtained by changing the primary to secondary mirror spacing.

* Simplify testing, including providing a capability to focus on point test sources as close as 100 meters.

The focus adjustment was implemented with a mechanism that moves the field stop and collimating lens assembly on a lead screw. Spring plungers in the tube surrounding the field stop and collimating lens assembly minimize lateral image shift during focus adjustment.

## 7. LESSONS LEARNED

### 7.1. Telescope Design

Early in the project a Dall-Kirkham telescope was considered, expecting that the cost of producing an aspheric secondary mirror would exceed the savings from the use of a paraboloidal primary mirror. Cost comparisons with various potential vendors did not bear this out, so a traditional Cassegrain telescope was used for the improved performance over the field. In retrospect, it may have been better to stay with the Dall-Kirkham design because of its relative simplicity in achieving and maintaining alignment. A spherical secondary mirror only had three degrees of freedom, which can be accomplished completely by x, y and z displacements. By comparison, the hyperboloidal secondary mirror of the Cassegrain telescope has tip and tilt of the secondary in addition to the other degrees of freedom listed above. This vastly complicates the alignment algorithm. For an instrument which might have to have its own internal automated alignment system, the Dall-Kirkham telescope may prove to be much simpler to employ.

### 7.2. Lens Selection

The gradient index lens chosen for collimation of the laser is probably not the best choice. While the optical performance is excellent, and the lens provides a small profile and is available at a modest price, there are concerns regarding the lens performance in the space radiation environment. Relatively little data is available on this in the open literature. Whereas the manufacturer indicates that special radiation-tolerant lenses can be made, they are not a stock item. A single custom asphere could also meet the requirements easily, and could be made using radiation tolerant glass from the beginning.

### 7.3. Configuration Control

Proper configuration control and the use of formal interface control documentation add considerable cost and complexity to a project, and results in significant schedule extension. However, it is generally agreed that it saves on design and rework cost in the long run. Some degree of configuration control and interface control were employed in this project, to the project's benefit: a library was established early in the project to make the latest optical designs available to the mechanical designers. While interface control documentation was developed, in a few cases efforts to meet the aggressive schedule resulted in the interface control documentation not being rigorously followed. This resulted in some rework.

## 8. CONCLUSIONS

A compact, self-contained functional optical transceiver system has been designed and developed to meet the technical requirements of transmitting multiple Mb/s from Mars to Earth. Initial imperfections in the manufacture of the instrument's optics were diagnosed and corrected to bring the system to diffraction-limited performance. Where practical, off-the-shelf components were used to facilitate the aggressive cost and schedule goals for this development project. In almost all cases, flight-like components were used to assure development of a system that can be fielded when the opportunity arises.

In addition to the valuable experience gained in the design, development and integration of this complex instrument, this effort developed a prototype which can be used for design evaluation, testing the limits of the system's performance, and evaluating the external link performance parameters so critical to future deep-space optical communication system design.

## ACKNOWLEDGEMENT

This work was carried out at the Jet Propulsion Laboratory, California Institute of Technology under contract with the National Aeronautics and Space Administration, and sponsored by the IND Technology program.

## REFERENCES

1. Hemmati, H., ed. [Deep Space Optical Communications], John Wiley & Sons, Hoboken, New Jersey, 14-23 (2006).
2. Lambert, S. G., Design and Analysis Study of a Spacecraft Optical Transceiver Package, Final Report – JPL Contract 957061, McDonnell Douglas Corp., St. Louis, MO, (1985)
3. Chen, C. and Lesh, J., "Overview of the Optical Communications Demonstrator", Proc. SPIE 2123, 85-95 (1994).
4. Jeganathan, M., Portillo, A., Racho, C. Lee, S., Erickson, D., DePew, J., Monacos, S. and Biswas, A., "Lessons Learnt from the Optical Communications Demonstrator (OCD)", Proc. SPIE 3615, 23-30 (1999).
5. Biswas, A., Wright, M. W., Sanii, B. and Page, N. A., 45 km Horizontal Path Optical Link Demonstrations", Proc. SPIE 4272, 60-71 (2001).
6. Boroson, D. M., Biswas, A., Edwards, B. L., "MLCD: overview of NASA's Mars laser communications system demonstration", Proc. SPIE 5338, 16-28 (2004).
7. Ortiz, G. G., Farr, W. H., , Roberts, W. T., Charles, J. R., Garkanian, W., Gin, J. Saharaspude, A., Piazzola, S., Sannibale, V. and Moison, B., "Canonical Deep-Space Optical Communications Transceiver", (7199) (2009).
8. Klein, B. J. and Degnan, J. J., "Optical Antenna Gain. 1: Transmitting Antennas", Applied Optics, 13(9), 2134-2141 (1974).